

Nociception-dependent CCL21 induce dorsal root ganglia axonal growth via CCR7-ERK activation

1 **Francina Mesquida-Veny^{1,2,3,4†}, Sara Martinez-Torres^{1,2,3,4†}, Jose Antonio Del Rio^{1,2,3,4}, Arnau
2 Hervera^{1,2,3,4*}**

3 ¹ Molecular and Cellular Neurobiotechnology, Institute for Bioengineering of Catalonia (IBEC),
4 Barcelona, Spain

5 ²Department of Cell Biology, Physiology and Immunology, University of Barcelona, Barcelona,
6 Spain

7 ³Network Centre of Biomedical Research of Neurodegenerative Diseases (CIBERNED), Institute of
8 Health Carlos III, ministry of Economy and Competitiveness, Madrid, Spain

9 ⁴Institute of Neuroscience, University of Barcelona, Barcelona, Spain

10 [†]These authors have contributed equally to this work and share first authorship

11 *** Correspondence:**

12 Corresponding Author

13 ahervera@ibecbarcelona.eu

14 **Keywords: CCL21, CCR7, MEK-ERK, axonal growth, actin.**

15 **Abstract**

16 While chemokines were originally described for their ability to induce cell migration, many studies
17 show how chemokines also take part in a variety of other cell functions, acting as adaptable
18 messengers in the communication between a diversity of cell types. In the nervous system,
19 chemokines participate both in physiological and pathological processes, and while their expression
20 is often described on glial and immune cells, growing evidence describe the expression of
21 chemokines and their receptors in neurons, highlighting, their potential in auto- and paracrine
22 signalling. In this study we analysed the role of nociception in the neuronal chemokinome, and their
23 role in axonal growth. We found that stimulating TRPV1⁺ nociceptors induces a transient increase in
24 CCL21. Interestingly we found that, this CCL21 increases neurite growth of large diameter
25 proprioceptors *in vitro*. Consistent with this, we show that proprioceptors express the CCL21
26 receptor CCR7, and a CCR7 neutralizing antibody dose-dependently attenuates CCL21-induced
27 neurite outgrowth. Mechanistically, we found that CCL21 binds locally to its receptor CCR7 at the
28 growth cone, activating the downstream MEK-ERK pathway, that in turn activates N-WASP,
29 triggering actin filament ramification in the growth cone, resulting in increased axonal growth.

30 **1 Introduction**

31 Classically, chemokines have been associated with leukocyte migration (1). Nevertheless, growing
32 evidence shows they can signal to a great variety of cell types and tissues (2,3). In addition, as
33 conventional chemokine receptors are G-protein coupled receptors (GPCRs), chemokines can initiate
34 a broad variety of intracellular signaling pathways (1).

Several studies have demonstrated the presence and the importance of chemokines in the nervous system (2,4,5). For instance, CXCL12 plays a vital role in regulating neuronal migration during cortical development (6,7). Remarkably, research is now showing neuronal expression of both chemokines and their receptors, suggesting an implication of these cells in direct neuronal communication (5,8)., In homeostasis, neuronal CX₃CL1 interacts with microglia preventing its activation (9). Additionally, neuronal chemokines have emerged as fundamental signals after insult, as for CCL2 or CCL21 among others (10–13), that are secreted upon neuronal injury and serve as chemoattractants of immune cells, triggering their activation and often leading to neuropathic pain (11–13). However, as in the case of CCL2 after peripheral injury, some chemokines have been also described to promote axonal regeneration as a result of macrophage recruitment and phenotype modulation (10,14). Meanwhile, although several chemokine receptors are expressed in different neuronal types (8,9), little is known about the functions chemokines may exert as autocrine or paracrine messengers on other neurons.

Neurons alter their secretome when exposed to different stimuli and according to their physiological state. In that direction, neuronal activity has shown to modulate neuronal communication, including with microglia or with other neurons beyond classical neurotransmission (15–17). Nociceptor activity after axonal injury is normally associated with pathological neuropathic pain (18), despite that, some studies have started to uncover how nociception participates in the healing process, such as promoting skin or adipose tissue regeneration, as well as neovascularization (19–21). These findings indicate that nociception might function as a key component of the healing machinery, and it is therefore important to study its precise roles in healing and regeneration in different tissues, including the nervous system.

In that sense, injured nociceptors have been described to release CCL21, however, whether this expression affected axonal regeneration has not been previously assessed (13). CCL21 has a primordial role in immune cell homing, via its canonical receptor CCR7 (22), but other functions for this chemokine in distinct tissues are also emerging, such as cartilage regeneration (23) and neuropathic pain induction in the CNS (13). Interestingly, in accordance with its function as a migration cue, the CCL21-CCR7 interaction activates intracellular pathways related to chemotaxis, via ERK signaling, this includes actin cytoskeleton remodeling via RhoA (24). Since cellular migration and growth cone dynamics are analogous mechanisms (25,26), we hypothesized that CCL21 could exert a growth promoting effect on neurons.

In the present study, we investigated the impact of nociceptor activation in the neuronal chemokinome which led us to find an undescribed mechanism of neuronal communication between two different neuronal types, nociceptors and proprioceptors. Specifically, we found that activation of TRPV1⁺ nociceptors induce an increase in CCL21 expression. Moreover, we revealed a novel role for this CCL21 in proprioceptors, promoting neurite outgrowth. We then found that the receptor CCR7, expressed in proprioceptors, was required for this effect, which was also dependent on the MEK-ERK pathway. Finally, our results disclose a local mechanism in the growth cone, where CCR7 expression is concentrated, affecting the actin cytoskeleton, ultimately leading to enhanced neurite outgrowth.

2 Materials and methods

76 Mice

77 B6.Cg-Tg(Thy1-COP4/EYFP)18Gfng/J (Thy1-ChR2) (27) were obtained from Jackson Laboratories
78 and C57BL/6J mice from Charles River Laboratories. PV-Cre/Ai27D/CSP-Flox mice (#008069 and
79 #012567 (Jackson Laboratories) crossbreeding) were provided by Dr. Rafael Fernández Chacón
80 (Instituto de Biomedicina de Sevilla, Spain). Mice ranging from 6-10 weeks were used. All animal
81 work was approved by the Ethics Committee on Animal Experimentation (CEEA) of the University
82 of Barcelona (procedures #276/16, 47/20, and OB41/21).

83 **Compounds**

84 Capsaicin (Merck, 100 μ g/ml i.pl.), CCL21 (Peprotech, 100ng/sciatic nerve *ex vivo*; 1nM, 10nM,
85 50nM *in vitro*), α CCR7 blocking antibody (R&D systems, 2-5 μ g/ml), rat immunoglobulin (Ig) G
86 (Merck, 2-5 μ g/ml), U0126 (Promega, 1 μ M), Wiskostatin (Merck, 1 μ M), CCL19 (Peprotech, 1 nM,
87 10nM, 50nM), Pertussis toxin (Merck, 50ng/ml).

88 ***In vitro* optogenetic stimulation**

89 Thy1-ChR2 DRG neurons were used for *in vitro* optogenetic stimulation. A 470nm emission LED
90 array (LuxeonRebelTM) under the control of a Driver LED (FemtoBuck, SparkFun) of 600mA and a
91 pulse generator PulsePal (OpenEphys)(28) was used to deliver blue light to neuronal cultures. The
92 optogenetic stimulation protocol consisted in 1h of illumination at 10Hz of frequency with 10ms-
93 90ms pulses, in 1s ON-4s OFF periods. Stimulation was applied 2h after seeding.

94 **Capsaicin administration**

95 Intraplantar (i.pl.) injection of capsaicin (10 μ l of 100 μ g/ml in PBS + 10% ethanol) was performed 2h
96 before animal sacrifice and DRG dissection.

97 **Dorsal root ganglia (DRG) neuronal culture**

98 DRGs were dissected, collected in ice-cold Hank's balanced salt solution (HBSS) (ThermoFisher
99 Scientific) and transferred to a digestion solution (5mg/ml Dispase II (Merck) and 2.5mg/ml
100 Collagenase Type II (ThermoFisher Scientific) in DMEM (ThermoFisher Scientific)) incubated for
101 45min at 37°C. DRGs were then centrifuged and digestion solution was then exchanged for
102 DMEM:F12 (ThermoFisher Scientific) media supplemented with 10% heat-inactivated FBS and 1x
103 B27 (ThermoFisher Scientific), the DRGs were then dissociated by pipetting. The resulting cell
104 suspension was then spun down, resuspended in culture media (DMEM:F-12 media supplemented
105 with 1x B27 and penicillin/streptomycin (P/S) (ThermoFisher Scientific)) and seeded in 48-well
106 plates (3000-4000 cells/well) previously coated with 0.1mg/ml poly-D-lysine (2h, 37°C; Merck) and
107 2 μ g/ml laminin (over-night (O/N), RT (room temperature); ThermoFisher Scientific). Cells were kept
108 at 37°C in a 5% CO₂ atmosphere.

109 Compounds were added 2h after plating, unless in combinatorial experiments, when blocking
110 antibodies or pharmacological inhibitors were added at 1,5h and the remaining compound 30 min
111 later. Cells were fixed 24h after the treatment.

112 **Local administration to the sciatic nerve and *ex vivo* DRG culture**

113 Mice were anaesthetized with inhaled isofluorane (4% induction, 2% maintenance). The sciatic nerve
114 was hooked and immobilized after skin incision and blunt dissection of the gluteus maximus and the
115 biceps femoralis. Compounds were locally injected into the nerve and the incision was closed by

116 layer. Animals were then allowed to recover for 24h. Sciatic DRGs (L4, L5, L6) were dissected and
117 processed for cell culture as previously explained.

118 **Immunocytochemistry**

119 Cells were fixed with cooled 4% paraformaldehyde (PFA) for 15min and washed in PBS (0.1M).
120 The cells were then blocked (PBS-0.25% Triton X-100+ 1% BSA (bovine serum albumin)) for 1h at
121 RT and then primary antibodies (anti- β III tubulin (Tuj1, 1:1000, BioLegend), anti-NFH (1:1000,
122 Merck), anti-CCR7 (1:200, Abcam)), were incubated O/N at 4°C in the same solution. After several
123 washes, Alexa-Fluor-conjugated secondary antibodies were incubated in blocking solution for 1h at
124 RT and cell nuclei were counterstained with Hoechst.

125 **Immunohistochemistry**

126 DRGs were dissected and fixed in PFA 4% for 2h at 4°C. After washing the DRGs were transferred
127 into cryoprotection solution (PBS-30% sucrose) for 24h at 4°C. Tissue freezing medium (OCT,
128 Merck) was used to freeze the DRGs in blocks, and then 10 μ m slices were generated with a cryostat
129 (Leica CM 1900) and mounted on slides. The slides were washed in TTBS (TBS (Tris-buffered
130 saline) + 1% Tween) and blocking solution (8% BSA and 0.3% Tx and 1/150 m α IgG (Jackson
131 Immuno Research)) was then incubated for 1h at RT. After an O/N incubation with primary
132 antibodies (anti-TRPV/VR1 (1:200, Santa Cruz), anti-CCL21 (1:200 Peprotech), anti-CCR7 (1:200,
133 Abcam)) in 2% BSA and 0.2% Tx in TBS at 4°C, and washing, Alexa-Fluor-conjugated secondary
134 antibodies were added in the same solution for 1h at RT. Preparations were then mounted with
135 coverslips in MowiolTM (Merck).

136 **Fluorescence intensity analysis**

137 DRG slices were stained for CCL21 and TRPV1. Images were acquired with a LSM 800 confocal
138 microscope (Zeiss) using an AxioCam 503c camera (Zeiss) at 20X magnification. Mean CCL21
139 fluorescence intensity (MFI) was computed in TRPV1⁺ cells using ImageJ, subtracting the
140 background for each image.

141 **Neurite length analysis**

142 Tuj1 immunocytochemistry was performed and imaged at 10X magnification using an Olympus
143 microscope IX71 with an Orca Flash 4 (3 images per well). The neurite length of large-diameter
144 (>35 μ m) neurons was blindly quantified with the Neuron J plugin for ImageJ (29). Average neurite
145 length per neuron was computed.

146 **Statistical analysis**

147 Statistics and graphical representation were carried out using Prism 6.0 (GraphPadTM Software).
148 Shapiro-Wilk test was used to verify normality of the distributions. * or # indicate significant
149 differences in ANOVA followed by Bonferroni's post-hoc test or Student's t-test. Plotted data
150 represents mean \pm s.e.m (standard error of the mean). All tests performed were two-sided, and
151 adjustments for multiple comparisons and/or significantly different variances (Fisher's F) were
152 applied were indicated. All data analysis was performed blind to the experimental group by two
153 independent experimenters. Unless otherwise stated, sample size was chosen in order to ensure a
154 power of at least 0.8, with a type I error threshold of 0.05, in view of the minimum effect size that
155 was expected.

156 **3 Results**

157 **3.1 CCL21 expression is upregulated upon nociceptor activation**

158 While most defined neuronal chemokines are induced after traumatic injury or inflammatory
159 signalling (30), we analysed whether stimulating neuronal activity in the DRG would have an impact
160 in chemokine expression and secretion. To this aim we used DRG neuronal cultures expressing ChR2
161 (from Thy1-ChR2 animals) and subjected them to optical stimulation. We recovered the media 24h
162 later and measured chemokine secretion using a Mouse Chemokine Array (Raybiotech).
163 Interestingly, we found a remarkable increase in CCL21 levels compared to non-stimulated controls
164 (Data not shown). ChR2 expression in DRGs is ubiquitous among all sensory subtypes (Fig 1A-B),
165 however, previous studies had reported CCL21 expression specifically in small diameter TRPV1⁺
166 nociceptors after peripheral nerve injury (31,32), so we hypothesized that this CCL21 increase after
167 optogenetic stimulation could be specific of this neuronal subtype. Accordingly, CCL21 expression
168 was increased in TRPV1⁺ nociceptors 2h after i.pl capsaicin (TRPV1 agonist) injection as compared
169 to vehicle administered animals (Student's T test $p= 0.0347$) (Fig. 1C-E).

170 **3.2 CCL21 promotes neurite outgrowth**

171 To test whether this chemokine could also influence axonal growth, we administered CCL21 into the
172 sciatic nerve and cultured disaggregated DRG neurons 24h after. This led to an increment in the
173 neurite outgrowth of *ex vivo* CCL21-treated DRG neurons when compared to vehicle treated ones
174 (Student's t-test $p= 0.0046$) (Fig. 2A-B). Additionally, administration of CCL21 at different doses
175 (1nM, 10nM, 50nM) on DRG cultures, resulted in a dose-dependent increase of DRG neurite
176 outgrowth *in vitro* (ANOVA followed by Bonferroni test; Veh vs 50nM $p= 0.0129$; 1nM vs 50nM $p=$
177 0.0440) (Fig. 2C-D).

178 **3.3 CCL21 activates proprioceptive CCR7 to promote neurite outgrowth**

179 CCL21 is a functional ligand of CCR7 (33). We therefore analysed the expression pattern of CCR7
180 in the DRG. We found CCR7 expression mainly in neurons, including in parvalbumin⁺ (PV) neurons,
181 that correspond to proprioceptors (Fig. 3A). Additionally, administering a CCR7-blocking antibody
182 to DRG cultures inhibited the neurite outgrowth induced by CCL21 as compared to the IgG control
183 (two-way ANOVA followed by Bonferroni test; interaction $p= 0.0233$; IgG-veh vs IgG-CCL21 $p=$
184 0.0055; IgG-CCL21 vs α CCR7 2 μ g-veh $p= 0.0040$; IgG-CCL21 vs α CCR7 2 μ g-CCL21 $p= 0.0355$;
185 IgG-CCL21 vs α CCR7 5 μ g-veh $p= 0.0037$; IgG-CCL21 vs α CCR7 5 μ g-CCL21 $p= 0.0079$) (Fig. 3B-
186 C). Parallelly, we tested whether CCL19, another CCR7 ligand(33), would induce the same effects.
187 Oppositely, CCL19 did not result in increased neurite outgrowth when administered *in vitro*
188 (Kruskal-Wallis test followed by Dunn's test; Veh vs 50nM $p > 0.9999$) (Supplementary Figure 1),
189 suggesting a CCL21 biased CCR7 activation is responsible for this particular mechanism.

190 **3.4 CCL21-CCR7 activates MEK-ERK pathway**

191 We then targeted the two main known downstream actuators of CCR7 activation, the MEK pathway
192 and the G_{i/o} protein previously known to be involved in axon growth(34–36)). Pharmacological
193 inhibition of MEK with U0126 blocks the neurite outgrowth induced by CCL21 (Fig. 4A-B), as
194 evidenced by the significant interaction of the treatments ($p= 0.0117$) on the two-way ANOVA
195 (multiple comparisons with Bonferroni test: DMSO-Veh vs DMSO-CCL21 $p= 0.0005$; DMSO-
196 CCL21 vs U0126-Veh $p= 0.0004$; DMSO-CCL21 vs U0126-CCL21 $p= 0.0001$). Conversely,
197 pertussis toxin (Ptx) administration, an inhibitor of the G_{i/o} protein did not affect the CCL21-induced

198 outgrowth (Supplementary Figure 2) as evidenced by the lack of significant interaction of the
199 treatments ($p= 0.7961$) on the two-way ANOVA (Student's t-test w/o (without) Ptx: $p= 0.0115$; with
200 Ptx: $p= 0.7458$).

201 **3.5 CCL21-CCR7-MEK pathway modulates actin cytoskeleton to promote neurite outgrowth**

202 Local assessment of the axonal tips revealed larger growth cones after CCL21 treatment (Fig. 5A),
203 this is in consonance with the especially abundant CCR7 expression found on these structures (Fig.
204 5B). We then sought to check the local effects that CCL21 could have in cytoskeletal dynamics of the
205 growth cones. Consequently, we inhibited actin branching by combining CCL21 administration with
206 wiskostatin, an inhibitor of the neural Wiskott-Aldrich syndrome protein (N-WASP), that acts as an
207 Arp2/3 complex activator. Wiskostatin co-administration greatly reduced the CCL21-induced
208 growth, supporting a local effect of CCL21 in the growth cone (two-way ANOVA followed by
209 Bonferroni test; interaction $p= 0.0825$; one-way ANOVA followed by Bonferroni test; DMSO-Veh
210 vs DMSO-CCL21 $p= 0.0207$; DMSO-CCL21 vs Wiskostatin-Veh $p= 0.0202$).

211 **4 Discussion**

212 There are plenty of evidence that neuronal activity can alter neuronal signalling. In that sense, we
213 found that the expression and release of the chemokine CCL21 is enhanced upon neuronal
214 stimulation. Interestingly, we found that specific TRPV1⁺ nociceptor stimulation is responsible for
215 CCL21 production, similarly to what has already been described upon axonal injury (31).

216 After axonal injury, release of neuronal CCL21 is mainly linked to neuropathic pain (13,37),
217 however, its role in axon growth and regeneration had never been described before. Interestingly, our
218 results revealed that CCL21 induces growth in proprioceptive neurons through activation of the
219 CCR7-MEK-ERK pathway, exerting an effect on actin dynamics at the growth cone level.

220 CCL21 was first designated as a recruiting cue for leucocytes, specifically stimulating the migration
221 of T cell subpopulations and dendritic cells (22,38–40). More recently, it has also been described to
222 induce migration in other cells such as tumorigenic or mesenchymal stem cells (41–45).
223 Fundamentally, cell migration and axonal growth are events that share similar cellular and molecular
224 machinery (46,47). Thus, molecules that orchestrate one process will most likely be implicated in the
225 other, and vice versa, as for instance what occurs with CXCL12 (48–51).

226 We also describe that CCL21 executes its growth-inducing function through its canonical receptor
227 CCR7, in accordance, we found abundant expression of this receptor on proprioceptive (PV⁺)
228 neurons, similarly to the findings of other studies, where neuronal CCR7 is abundantly found in
229 peripheral nerves and hippocampal neurons (52,53). Activation of CCR7 has already been shown to
230 play a cardinal role in the CCL21-induced cell migration (42,44,47,54,55), that, as stated, activates
231 similar cellular and molecular machinery than axonal growth (46,47).

232 Intriguingly, CCL19, another CCR7 ligand, did not induce axonal growth. This finding strengthens
233 the view of biased ligand-receptor responses, as already shown for CCL21 and CCL19, which can
234 trigger biased downstream effectors of CCR7 (56,57). These biased activations result in particular
235 mechanisms activated only by CCL21; however, this effect often varies depending on the target cell
236 (58–61).

237 We also found that pharmacological inhibition of the MEK-ERK pathway, one of the main
238 downstream mediators of CCR7 effects, inhibited the growth induced by CCL21. This goes in line

239 other studies defining MEK-ERK as the underlying mechanism of the chemotaxis induced by
240 CCL21-CCR7 (55,62). Contrarily, we did not see an effect by inhibiting the $G_{i/o}$ protein in the
241 CCL21- induced outgrowth, however lack of growth-suppression could derive from inactivation of
242 other growth-inhibitor pathways activated by the $G_{i/o}$ (63).

243 MEK-ERK pathway activation has been previously implicated in axonal regeneration (64–66). For
244 instance, after peripheral conditioning injury, ERK is phosphorylated and has been shown to affect
245 multiple cellular processes affecting axonal growth, including transcriptional and epigenetic
246 alterations, resulting increased expression of several regeneration associated genes (RAGs) (66),
247 increased retrograde transport (64,67) as well as stimulation of cytoskeleton dynamics (65).
248 According with the latter, ERK has been shown to have a direct effect on actin polymerization
249 (68,69), through phosphorylation of different effectors such as WAVE2, cortactin and Rac1 (70–74).
250 Remarkably, we found CCR7 expression to be particularly elevated in the growth cones, therefore,
251 we evaluated the effects of actin dynamics in the growth cone as a putative mechanism of the
252 CCL21-induced growth. In that sense, coadministration of an N-WASP pharmacological inhibitor, a
253 key actin polymerization component, blocked the growth induced by CCL21. N-WASP is an Arp2/3
254 complex activator, which in turn works as an actin-binding protein, mainly responsible for actin
255 filament branching (75). Previous studies already showed the essential role of Arp2/3 in growth cone
256 progression (76,77). Mechanistically, ERK is known to phosphorylate cortactin, leading to N-WASP
257 binding and activation (71). Thus, in a nutshell, we found that upon CCL21 binding to its receptor
258 CCR7 in the axonal growth cone, there is a downstream MEK-ERK activation, that leads to N-
259 WASP activation, triggering actin filament branching in this structure, resulting in increased axonal
260 growth (Figure 6).

261 While CCL21 has been already described for its role in regeneration in other tissues including skin,
262 cartilage, and vascular remodelling (41,43,78), here we describe a novel role of this chemokine in
263 axonal growth.

264 Additionally, the mechanism described involves an unprecedented paracrine dialogue based on
265 chemokines between two different DRG neuronal types. While neurons are highly interconnected
266 through synapses, there is little work regarding other forms of neuronal communication (79). Growth
267 factors, for instance, have been implicated in both paracrine and autocrine neuronal communication
268 (80–83), however, we describe a novel chemokine dependant mechanism of neuron-neuron
269 signalling.

270 Parallelly, we have also unravelled a novel role of nociceptive signalling in sensory axon
271 regeneration. Nociception and pain are tightly associated with tissue injury (84,85), and while it is
272 not surprising that a signal initiated by an injury could trigger the healing process, after nerve injury
273 chemokine release and nociceptor activity have been typically linked to pathological neuropathic
274 pain. Contrarily, here we show that stimulating nociceptor activity triggers the secretion of a growth-
275 promoting chemokine, CCL21. In agreement with this, nociceptive signalling participates in the
276 healing cascade of several tissues, for example, nociceptor activation induces adipose tissue
277 regeneration through CGRP (calcitonin gene-related peptide) secretion (86), angiogenesis via
278 Substance-P-mediated effects (87), and skin regeneration through modulation of the immune
279 response (88). Pain and nociceptive signalling are complex evolutionary mechanisms that might have
280 further implications than previously anticipated, as they play central roles orchestrating and
281 promoting the healing process in different tissues.

282 This also suggest caution in the indiscriminate use of analgesic drugs and treatments after injury, as
283 these may hinder nociceptive regenerative signalling, limiting the healing process, similarly to the
284 effects observed by broad immunosuppressive drugs (89) or antioxidants (90) after SCIs. Therefore,
285 appropriate timing and level of analgesic inhibition after injury will likely need to be tailored to
286 provide pain relief while avoiding unwanted effects in hindering the tissue regeneration. An
287 additional intriguing implication is the possibility to modulate nociceptive signalling to achieve tissue
288 regeneration. While therapeutically, inducing nociception is not a reasonable approach, further
289 investigation and characterization of signalling elicited by nociceptor stimulation may increase our
290 understanding of the molecular mechanisms underlying the healing process, and may enable the
291 future design of therapeutic targets and strategies to foster tissue regeneration.

292 **5 Conflict of Interest**

293 The authors declare that the research was conducted in the absence of any commercial or financial
294 relationships that could be construed as a potential conflict of interest.

295 **6 Author Contributions**

296 FMV performed, designed experiments, performed data analysis, and wrote the manuscript; SMT
297 performed and designed experiments and performed data analysis; JADR supervised experiments,
298 provided experimental funds and edited the manuscript; AH performed, designed experiments,
299 performed data analysis, provided experimental funds and wrote the manuscript.

300 **7 Funding**

301 This research was supported by HDAC3-EAE-SCI Project with ref. PID2020-119769RA-I00 from
302 MCIN/ AEI /10.13039/501100011033 to AH and PRPSEM Project with ref. RTI2018-099773-B-I00
303 from MCINN/AEI/10.13039/501100011033/ FEDER “Una manera de hacer Europa”, the CERCA
304 Programme, and the Commission for Universities and Research of the Department of Innovation,
305 Universities, and Enterprise of the Generalitat de Catalunya (SGR2017-648) to JADR. The project
306 leading to these results received funding from the María de Maeztu Unit of Excellence (Institute of
307 Neurosciences, University of Barcelona) MDM-2017-0729 and Severo Ochoa Unit of Excellence
308 (Institute of Bioengineering of Catalonia) CEX2018-000789-S from MCIN/AEI
309 /10.13039/501100011033. FMV was supported by a fellowship from the “Ayudas para la Formación
310 de Profesorado Universitario” (FPU16/03992) program, from the Spanish Ministry of Universities.

311 **8 Acknowledgments**

312 The authors thank Miriam Segura-Feliu for her technical help. PV-Cre/Ai27D/CSP-Flox mice
313 (#008069 and #012567 (Jackson Laboratories) crossbreeding) were generated and provided by Dr.
314 Rafael Fernández-Chacón (Instituto de Biomedicina de Sevilla).

315 **9 References**

- 316 1. Hughes CE, Nibbs RJB. A guide to chemokines and their receptors. *FEBS Journal* (2018)
317 **285**:2944–2971. doi: 10.1111/febs.14466
- 318 2. Jaerve A, Müller HW. Chemokines in CNS injury and repair. *Cell and Tissue Research* (2012)
319 doi: 10.1007/s00441-012-1427-3

320 3. Anders HJ, Romagnani P, Mantovani A. Pathomechanisms: Homeostatic chemokines in
321 health, tissue regeneration, and progressive diseases. *Trends in Molecular Medicine* (2014)
322 **20**:154–165. doi: 10.1016/j.molmed.2013.12.002

323 4. De Haas AH, Van Weering HRJ, De Jong EK, Boddeke HWGM, Biber KPH. Neuronal
324 chemokines: Versatile messengers in central nervous system cell interaction. *Molecular*
325 *Neurobiology* (2007) doi: 10.1007/s12035-007-0036-8

326 5. Mesquida-Veny F, Del Río JA, Hervera A. Macrophagic and microglial complexity after
327 neuronal injury. *Progress in Neurobiology* (2021) **200**: doi: 10.1016/j.pneurobio.2020.101970

328 6. Borrell V, Marín O. Meninges control tangential migration of hem-derived Cajal-Retzius cells
329 via CXCL12/CXCR4 signaling. *Nature Neuroscience* (2006) **9**:1284–1293. doi:
330 10.1038/nn1764

331 7. Lysko DE, Putt M, Golden JA. SDF1 regulates leading process branching and speed of
332 migrating interneurons. *Journal of Neuroscience* (2011) **31**:1739–1745. doi:
333 10.1523/JNEUROSCI.3118-10.2011

334 8. Cartier L, Hartley O, Dubois-Dauphin M, Krause KH. Chemokine receptors in the central
335 nervous system: Role in brain inflammation and neurodegenerative diseases. *Brain Research*
336 *Reviews* (2005) **48**:16–42. doi: 10.1016/j.brainresrev.2004.07.021

337 9. Williams JL, Holman DW, Klein RS. Chemokines in the balance: Maintenance of homeostasis
338 and protection at CNS barriers. *Frontiers in Cellular Neuroscience* (2014) doi:
339 10.3389/fncel.2014.00154

340 10. Kwon MJ, Shin HY, Cui Y, Kim H, Le Thi AH, Choi JY, Kim EY, Hwang DH, Kim BG.
341 CCL2 mediates neuron-macrophage interactions to drive proregenerative macrophage
342 activation following preconditioning injury. *Journal of Neuroscience* (2015) doi:
343 10.1523/JNEUROSCI.1924-15.2015

344 11. Hu Z, Deng N, Liu K, Zeng W. DLK mediates the neuronal intrinsic immune response and
345 regulates glial reaction and neuropathic pain. *Experimental Neurology* (2019) doi:
346 10.1016/j.expneurol.2019.113056

347 12. Wang Q, Zhang S, Liu T, Wang H, Liu K, Wang Q, Zeng W. Sarm1/Myd88-5 Regulates
348 Neuronal Intrinsic Immune Response to Traumatic Axonal Injuries. *Cell Reports* (2018) doi:
349 10.1016/j.celrep.2018.03.071

350 13. Biber K, Tsuda M, Tozaki-Saitoh H, Tsukamoto K, Toyomitsu E, Masuda T, Boddeke H,
351 Inoue K. Neuronal CCL21 up-regulates microglia P2X4 expression and initiates neuropathic
352 pain development. *EMBO Journal* (2011) doi: 10.1038/emboj.2011.89

353 14. Bhardwaj D, Náger M, Camats J, David M, Benguria A, Dopazo A, Cantí C, Herreros J.
354 Chemokines induce axon outgrowth downstream of hepatocyte growth factor and TCF/β-
355 catenin signaling. *Frontiers in Cellular Neuroscience* (2013) doi: 10.3389/fncel.2013.00052

356 15. Park S, Koppes RA, Froriep UP, Jia X, Achyuta AKH, McLaughlin BL, Anikeeva P.
357 Optogenetic control of nerve growth. *Scientific Reports* (2015) **5**:1–9. doi: 10.1038/srep09669

358 16. Ferro A, Auguste YSS, Cheadle L. Microglia, Cytokines, and Neural Activity: Unexpected
359 Interactions in Brain Development and Function. *Frontiers in Immunology* (2021) **12**:1–14.
360 doi: 10.3389/fimmu.2021.703527

361 17. Nguyen PT, Dorman LC, Pan S, Vainchtein ID, Han RT, Nakao-Inoue H, Taloma SE, Barron
362 JJ, Molofsky AB, Kheirbek MA, et al. Microglial Remodeling of the Extracellular Matrix
363 Promotes Synapse Plasticity. *Cell* (2020) **182**:388–403.e15. doi: 10.1016/j.cell.2020.05.050

364 18. Costigan M, Scholz J, Woolf CJ. Neuropathic pain: A maladaptive response of the nervous
365 system to damage. *Annual Review of Neuroscience* (2009) **32**:1–32. doi:
366 10.1146/annurev.neuro.051508.135531

367 19. Amadesi S, Reni C, Katare R, Meloni M, Oikawa A, Beltrami AP, Avolio E, Cesselli D,
368 Fortunato O, Spinetti G, et al. Role for substance P-based nociceptive signaling in progenitor
369 cell activation and angiogenesis during ischemia in mice and in human subjects. *Circulation*
370 (2012) **125**:1774–1786. doi: 10.1161/CIRCULATIONAHA.111.089763

371 20. Rabiller L, Labit E, Guissard C, Gilardi S, Guiard BP, Moulédous L, Silva M, Mithieux G,
372 Pénicaud L, Lorsignol A, et al. Pain sensing neurons promote tissue regeneration in adult
373 mice. *npj Regenerative Medicine* (2021) **6**:1–9. doi: 10.1038/s41536-021-00175-7

374 21. Wei JJ, Kim HS, Spencer CA, Brennan-Crispi D, Zheng Y, Johnson NM, Rosenbach M,
375 Miller C, Leung DH, Cotsarelis G, et al. Activation of TRPA1 nociceptor promotes systemic
376 adult mammalian skin regeneration. *Science Immunology* (2020) **5**:1–9. doi:
377 10.1126/SCIIMMUNOL.ABA5683

378 22. Förster R, Davalos-Misslitz AC, Rot A. CCR7 and its ligands: Balancing immunity and
379 tolerance. *Nature Reviews Immunology* (2008) **8**:362–371. doi: 10.1038/nri2297

380 23. Joutoku Z, Onodera T, Matsuoka M, Homan K, Momma D, Baba R, Hontani K, Hamasaki M,
381 Matsubara S, Hishimura R, et al. CCL21/CCR7 axis regulating juvenile cartilage repair can
382 enhance cartilage healing in adults. *Scientific Reports* (2019) **9**:1–12. doi: 10.1038/s41598-
383 019-41621-3

384 24. Rodríguez-Fernández JL, Criado-García O. The Chemokine Receptor CCR7 Uses Distinct
385 Signaling Modules With Biased Functionality to Regulate Dendritic Cells. *Frontiers in
386 Immunology* (2020) **11**:1–10. doi: 10.3389/fimmu.2020.00528

387 25. Aberle H. Axon guidance and collective cell migration by substrate-derived attractants.
388 *Frontiers in Molecular Neuroscience* (2019) **12**:1–7. doi: 10.3389/fnmol.2019.00148

389 26. Cooper JA. Mechanisms of cell migration in the nervous system. *Journal of Cell Biology*
390 (2013) **202**:725–734. doi: 10.1083/jcb.201305021

391 27. Arenkiel BR, Peca J, Davison IG, Feliciano C, Deisseroth K, Augustine GJJ, Ehlers MD, Feng
392 G. In Vivo Light-Induced Activation of Neural Circuitry in Transgenic Mice Expressing
393 Channelrhodopsin-2. *Neuron* (2007) **54**: doi: 10.1016/j.neuron.2007.03.005

394 28. Siegle JH, López AC, Patel YA, Abramov K, Ohayon S, Voigts J. Open Ephys: An open-
395 source, plugin-based platform for multichannel electrophysiology. *Journal of Neural*
396 *Engineering* (2017) **14**: doi: 10.1088/1741-2552/aa5eea

397 29. Meijering E, Jacob M, Sarria JCF, Steiner P, Hirling H, Unser M. Design and Validation of a
398 Tool for Neurite Tracing and Analysis in Fluorescence Microscopy Images. *Cytometry Part A*
399 (2004) **58**: doi: 10.1002/cyto.a.20022

400 30. Mesquida-Veny F, del Río JA, Hervera A. Macrophagic and microglial complexity after
401 neuronal injury. *Progress in Neurobiology* (2021) **200**: doi: 10.1016/j.pneurobio.2020.101970

402 31. Biber K, Tsuda M, Tozaki-Saitoh H, Tsukamoto K, Toyomitsu E, Masuda T, Boddeke H,
403 Inoue K. Neuronal CCL21 up-regulates microglia P2X4 expression and initiates neuropathic
404 pain development. *EMBO Journal* (2011) doi: 10.1038/emboj.2011.89

405 32. Zhao P, Waxman SG, Hains BC. Modulation of thalamic nociceptive processing after spinal
406 cord injury through remote activation of thalamic microglia by cysteine-cysteine chemokine
407 ligand 21. *Journal of Neuroscience* (2007) doi: 10.1523/JNEUROSCI.2209-07.2007

408 33. Yoshida R, Nagira M, Kitaura M, Imagawa N, Imai T, Yoshie O. Secondary lymphoid-tissue
409 chemokine is a functional ligand for the CC chemokine receptor CCR7. *Journal of Biological*
410 *Chemistry* (1998) **273**: doi: 10.1074/jbc.273.12.7118

411 34. Hasegawa Y, Fujitani M, Hata K, Tohyama M, Yamagishi S, Yamashita T. Promotion of axon
412 regeneration by myelin-associated glycoprotein and Nogo through divergent signals
413 downstream of Gi/G. *Journal of Neuroscience* (2004) **24**:6826–6832. doi:
414 10.1523/JNEUROSCI.1856-04.2004

415 35. Perlson E, Hanz S, Ben-Yaakov K, Segal-Ruder Y, Seger R, Fainzilber M. Vimentin-
416 dependent spatial translocation of an activated MAP kinase in injured nerve. *Neuron* (2005)
417 **45**:715–726. doi: 10.1016/j.neuron.2005.01.023

418 36. Chierzi S, Ratto GM, Verma P, Fawcett JW. The ability of axons to regenerate their growth
419 cones depends on axonal type and age, and is regulated by calcium, cAMP and ERK.
420 *European Journal of Neuroscience* (2005) **21**:2051–2062. doi: 10.1111/j.1460-
421 9568.2005.04066.x

422 37. De Jong EK, Dijkstra IM, Hensens M, Brouwer N, Van Amerongen M, Liem RSB, Boddeke
423 HWGM, Biber K. Vesicle-mediated transport and release of CCL21 in endangered neurons: A
424 possible explanation for microglia activation remote from a primary lesion. *Journal of*
425 *Neuroscience* (2005) doi: 10.1523/JNEUROSCI.1019-05.2005

426 38. Shannon LA, Calloway PA, Welch TP, Vines CM. CCR7/CCL21 migration on fibronectin is
427 mediated by phospholipase C γ 1 and ERK1/2 in primary T lymphocytes. *Journal of Biological*
428 *Chemistry* (2010) **285**:38781–38787. doi: 10.1074/jbc.M110.152173

429 39. Britschgi MR, Favre S, Luther SA. CCL21 is sufficient to mediate DC migration, maturation
430 and function in the absence of CCL19. *European Journal of Immunology* (2010) **40**:1266–
431 1271. doi: 10.1002/eji.200939921

432 40. Scandella E, Men Y, Legler DF, Gillessen S, Prikler L, Ludewig B, Groettrup M.
433 CCL19/CCL21-triggered signal transduction and migration of dendritic cells requires
434 prostaglandin E2. *Blood* (2004) **103**:1595–1601. doi: 10.1182/blood-2003-05-1643

435 41. Joutoku Z, Onodera T, Matsuoka M, Homan K, Momma D, Baba R, Hontani K, Hamasaki M,
436 Matsubara S, Hishimura R, et al. CCL21/CCR7 axis regulating juvenile cartilage repair can
437 enhance cartilage healing in adults. *Scientific Reports* (2019) **9**:1–12. doi: 10.1038/s41598-
438 019-41621-3

439 42. Li F, Zou Z, Suo N, Zhang Z, Wan F, Zhong G, Qu Y, Ntaka KS, Tian H. CCL21/CCR7 axis
440 activating chemotaxis accompanied with epithelial–mesenchymal transition in human breast
441 carcinoma. *Medical Oncology* (2014) **31**:1–10. doi: 10.1007/s12032-014-0180-8

442 43. Sasaki M, Abe R, Fujita Y, Ando S, Inokuma D, Shimizu H. Mesenchymal Stem Cells Are
443 Recruited into Wounded Skin and Contribute to Wound Repair by Transdifferentiation into
444 Multiple Skin Cell Type. *The Journal of Immunology* (2008) **180**:2581–2587. doi:
445 10.4049/jimmunol.180.4.2581

446 44. Mo M, Zhou M, Wang L, Qi L, Zhou K, Liu LF, Chen Z, Zu XB. CCL21/CCR7 enhances the
447 proliferation, migration, and invasion of human bladder cancer T24 cells. *PLoS ONE* (2015)
448 **10**:1–12. doi: 10.1371/journal.pone.0119506

449 45. Xiong Y, Huang F, Li X, Chen Z, Feng D, Jiang H, Chen W, Zhang X. CCL21/CCR7
450 interaction promotes cellular migration and invasion via modulation of the MEK/ERK1/2
451 signaling pathway and correlates with lymphatic metastatic spread and poor prognosis in
452 urinary bladder cancer. *International Journal of Oncology* (2017) **51**:75–90. doi:
453 10.3892/ijo.2017.4003

454 46. Aberle H. Axon guidance and collective cell migration by substrate-derived attractants.
455 *Frontiers in Molecular Neuroscience* (2019) **12**:1–7. doi: 10.3389/fnmol.2019.00148

456 47. Cooper JA. Mechanisms of cell migration in the nervous system. *Journal of Cell Biology*
457 (2013) **202**:725–734. doi: 10.1083/jcb.201305021

458 48. Borrell V, Marín O. Meninges control tangential migration of hem-derived Cajal-Retzius cells
459 via CXCL12/CXCR4 signaling. *Nature Neuroscience* (2006) **9**:1284–1293. doi:
460 10.1038/nn1764

461 49. Doitsidou M, Reichman-Fried M, Stebler J, Köprunner M, Dörries J, Meyer D, Esguerra C v,
462 Leung TC, Raz E. Guidance of primordial germ cell migration by the chemokine SDF-1. *Cell*
463 (2002) **111**:647–659. doi: 10.1016/S0092-8674(02)01135-2

464 50. Opatz J, Küry P, Schiwy N, Järve A, Estrada V, Brazda N, Bosse F, Müller HW. SDF-1
465 stimulates neurite growth on inhibitory CNS myelin. *Molecular and Cellular Neuroscience*
466 (2009) doi: 10.1016/j.mcn.2008.11.002

467 51. Pujol F, Kitabgi P, Boudin H. The chemokine SDF-1 differentially regulates axonal elongation
468 and branching in hippocampal neurons. *Journal of Cell Science* (2005) **118**:1071–1080. doi:
469 10.1242/jcs.01694

470 52. Hirth M, Gandla J, Höper C, Gaida MM, Agarwal N, Simonetti M, Demir A, Xie Y, Weiss C,
471 Michalski CW, et al. CXCL10 and CCL21 Promote Migration of Pancreatic Cancer Cells
472 Toward Sensory Neurons and Neural Remodeling in Tumors in Mice, Associated With Pain in
473 Patients. *Gastroenterology* (2020) **159**:665-681.e13. doi: 10.1053/j.gastro.2020.04.037

474 53. Liu JX, Cao X, Tang YC, Liu Y, Tang FR. CCR7, CCR8, CCR9 and CCR10 in the mouse
475 hippocampal CA1 area and the dentate gyrus during and after pilocarpine-induced status
476 epilepticus. *Journal of Neurochemistry* (2007) **100**:1072–1088. doi: 10.1111/j.1471-
477 4159.2006.04272.x

478 54. Comerford I, Harata-Lee Y, Bunting MD, Gregor C, Kara EE, McColl SR. A myriad of
479 functions and complex regulation of the CCR7/CCL19/CCL21 chemokine axis in the adaptive
480 immune system. *Cytokine and Growth Factor Reviews* (2013) **24**:269–283. doi:
481 10.1016/j.cytofr.2013.03.001

482 55. Shannon LA, Calloway PA, Welch TP, Vines CM. CCR7/CCL21 migration on fibronectin is
483 mediated by phospholipase C γ 1 and ERK1/2 in primary T lymphocytes. *Journal of Biological
484 Chemistry* (2010) **285**:38781–38787. doi: 10.1074/jbc.M110.152173

485 56. Hauser MA, Legler DF. Common and biased signaling pathways of the chemokine receptor
486 CCR7 elicited by its ligands CCL19 and CCL21 in leukocytes. *Journal of Leukocyte Biology*
487 (2016) **99**:869–882. doi: 10.1189/jlb.2mr0815-380r

488 57. Jørgensen AS, Rosenkilde MM, Hjortø GM. Biased signaling of G protein-coupled receptors –
489 From a chemokine receptor CCR7 perspective. *General and Comparative Endocrinology*
490 (2018) **258**:4–14. doi: 10.1016/j.ygcen.2017.07.004

491 58. Hjortø GM, Larsen O, Steen A, Daugvilaite V, Berg C, Fares S, Hansen M, Ali S, Rosenkilde
492 MM. Differential CCR7 targeting in dendritic cells by three naturally occurring CC-
493 chemokines. *Frontiers in Immunology* (2016) **7**:1–15. doi: 10.3389/fimmu.2016.00568

494 59. Corbisier J, Galès CL, Huszagh A, Parmentier M, Springael JY. Biased signaling at
495 chemokine receptors. *Journal of Biological Chemistry* (2015) **290**:9542–9554. doi:
496 10.1074/jbc.M114.596098

497 60. Kohout TA, Nicholas SL, Perry SJ, Reinhart G, Junger S, Struthers RS. Differential
498 desensitization, receptor phosphorylation, β -arrestin recruitment, and ERK1/2 activation by the
499 two endogenous ligands for the CC chemokine receptor 7. *Journal of Biological Chemistry*
500 (2004) **279**:23214–23222. doi: 10.1074/jbc.M402125200

501 61. Shannon LA, McBurney TM, Wells MA, Roth ME, Calloway PA, Bill CA, Islam S, Vines
502 CM. CCR7/CCL19 controls expression of EDG-1 in T cells. *Journal of Biological Chemistry*
503 (2012) **287**:11656–11664. doi: 10.1074/jbc.M111.310045

504 62. Riol-Blanco L, Sánchez-Sánchez N, Torres A, Tejedor A, Narumiya S, Corbí AL, Sánchez-
505 Mateos P, Rodríguez-Fernández JL. The Chemokine Receptor CCR7 Activates in Dendritic
506 Cells Two Signaling Modules That Independently Regulate Chemotaxis and Migratory Speed.
507 *The Journal of Immunology* (2005) **174**:4070–4080. doi: 10.4049/jimmunol.174.7.4070

508 63. Cai D, Yingjing S, de Bellard ME, Tang S, Filbin MT. Prior exposure to neurotrophins blocks
509 inhibition of axonal regeneration by MAG and myelin via a cAMP-dependent mechanism.
510 *Neuron* (1999) **22**: doi: 10.1016/S0896-6273(00)80681-9

511 64. Perlson E, Hanz S, Ben-Yaakov K, Segal-Ruder Y, Seger R, Fainzilber M. Vimentin-
512 dependent spatial translocation of an activated MAP kinase in injured nerve. *Neuron* (2005)
513 **45**: doi: 10.1016/j.neuron.2005.01.023

514 65. Chierzi S, Ratto GM, Verma P, Fawcett JW. The ability of axons to regenerate their growth
515 cones depends on axonal type and age, and is regulated by calcium, cAMP and ERK.
516 *European Journal of Neuroscience* (2005) **21**: doi: 10.1111/j.1460-9568.2005.04066.x

517 66. Puttagunta R, Tedeschi A, Sória MG, Hervera A, Lindner R, Rathore KI, Gaub P, Joshi Y,
518 Nguyen T, Schmandke A, et al. PCAF-dependent epigenetic changes promote axonal
519 regeneration in the central nervous system. *Nature Communications* (2014) **5**: doi:
520 10.1038/ncomms4527

521 67. Hanz S, Fainzilber M. Retrograde signaling in injured nerve - The axon reaction revisited.
522 *Journal of Neurochemistry* (2006) **99**: doi: 10.1111/j.1471-4159.2006.04089.x

523 68. Leite SC, Pinto-Costa R, Sousa MM. Actin dynamics in the growth cone: a key player in axon
524 regeneration. *Current Opinion in Neurobiology* (2021) **69**:11–18. doi:
525 10.1016/j.conb.2020.11.015

526 69. Tanimura S, Takeda K. ERK signalling as a regulator of cell motility. *Journal of Biochemistry*
527 (2017) **162**:145–154. doi: 10.1093/jb/mvx048

528 70. Danson CM, Pocha SM, Bloomberg GB, Cory GO. Phosphorylation of WAVE2 by MAP
529 kinases regulates persistent cell migration and polarity. *Journal of Cell Science* (2007)
530 **120**:4144–4154. doi: 10.1242/jcs.013714

531 71. Martinez-Quiles N, Ho H-YH, Kirschner MW, Ramesh N, Geha RS. Erk/Src Phosphorylation
532 of Cortactin Acts as a Switch On-Switch Off Mechanism That Controls Its Ability To Activate
533 N-WASP. *Molecular and Cellular Biology* (2004) **24**:5269–5280. doi:
534 10.1128/mcb.24.12.5269-5280.2004

535 72. Mendoza MC, Er EE, Zhang W, Ballif BA, Elliott HL, Danuser G, Blenis J. ERK-MAPK
536 Drives Lamellipodia Protrusion by Activating the WAVE2 Regulatory Complex. *Molecular
537 Cell* (2011) **41**:661–671. doi: 10.1016/j.molcel.2011.02.031

538 73. Nakanishi O, Suetsugu S, Yamazaki D, Takenawa T. Effect of WAVE2 phosphorylation on
539 activation of the Arp2/3 complex. *Journal of Biochemistry* (2007) **141**:319–325. doi:
540 10.1093/jb/mvm034

541 74. Tong J, Li L, Ballermann B, Wang Z. Phosphorylation of Rac1 T108 by Extracellular Signal-
542 Regulated Kinase in Response to Epidermal Growth Factor: a Novel Mechanism To Regulate
543 Rac1 Function. *Molecular and Cellular Biology* (2013) **33**:4538–4551. doi:
544 10.1128/mcb.00822-13

545 75. Pollard TD. Actin and actin-binding proteins. *Cold Spring Harbor Perspectives in Biology*
546 (2016) **8**:1–17. doi: 10.1101/cshperspect.a018226

547 76. Ruiz-Miguel JES, Letourneau PC. The role of Arp2/3 in growth cone actin dynamics and
548 guidance is substrate dependent. *Journal of Neuroscience* (2014) **34**:5895–5908. doi:
549 10.1523/JNEUROSCI.0672-14.2014

550 77. Schlau M, Terheyden-Keighley D, Theis V, Mannherz HG, Theiss C. VEGF triggers the
551 activation of cofilin and the Arp2/3 complex within the growth cone. *International Journal of*
552 *Molecular Sciences* (2018) **19**: doi: 10.3390/ijms19020384

553 78. Nossent AY, Bastiaansen AJNM, Peters EAB, de Vries MR, Aref Z, Welten SMJ, de Jager
554 SCA, van der Pouw Kraan TCTM, Quax PHA. CCR7-CCL19/CCL21 axis is essential for
555 effective arteriogenesis in a murine model of hindlimb ischemia. *Journal of the American*
556 *Heart Association* (2017) **6**:1–17. doi: 10.1161/JAHA.116.005281

557 79. Herrmann KA, Broihier HT. What neurons tell themselves: autocrine signals play essential
558 roles in neuronal development and function. *Current Opinion in Neurobiology* (2018) **51**:70–
559 79. doi: 10.1016/j.conb.2018.03.002

560 80. Acheson A, Conover JC, Fandl JP, DeChiara TM, Russell M, Thadani A, Squinto SP,
561 Yancopoulos GD, Lindsay RM. A BDNF autocrine loop in adult sensory neurons prevents cell
562 death. *Nature (London)* (1995) **374**:450–453. doi: 10.1038/374450a0

563 81. Cheng PL, Song AH, Wong YH, Wang S, Zhang X, Poo MM. Self-amplifying autocrine
564 actions of BDNF in axon development. *Proceedings of the National Academy of Sciences of*
565 *the United States of America* (2011) **108**:18430–18435. doi: 10.1073/pnas.1115907108

566 82. Froger N, Matonti F, Roubeix C, Forster V, Ivkovic I, Brunel N, Baudouin C, Sahel JA,
567 Picaud S. VEGF is an autocrine/paracrine neuroprotective factor for injured retinal ganglion
568 neurons. *Scientific Reports* (2020) **10**:1–11. doi: 10.1038/s41598-020-68488-z

569 83. Ogunshola OO, Antic A, Donoghue MJ, Fan SY, Kim H, Stewart WB, Madri JA, Ment LR.
570 Paracrine and autocrine functions of neuronal vascular endothelial growth factor (VEGF) in
571 the central nervous system. *Journal of Biological Chemistry* (2002) **277**:11410–11415. doi:
572 10.1074/jbc.M111085200

573 84. Baliki MN, Apkarian AV. Nociception, Pain, Negative Moods, and Behavior Selection.
574 *Neuron* (2015) **87**:474–491. doi: 10.1016/j.neuron.2015.06.005

575 85. Woller SA, Eddinger KA, Corr M, Yaksh TL, Corr M, Yaksh TL. Woller S.A, Eddinger K.A.,
576 Corr M, Yaksh T.L, An overview of pathways encoding nociception. *Clin Exp Rheumatol*
577 2017; 35 (suppl. 107) S40-S46. (2017)

578 86. Rabiller L, Labit E, Guissard C, Gilardi S, Guiard BP, Moulédous L, Silva M, Mithieux G,
579 Pénaud L, Lorsignol A, et al. Pain sensing neurons promote tissue regeneration in adult
580 mice. *npj Regenerative Medicine* (2021) **6**:1–9. doi: 10.1038/s41536-021-00175-7

581 87. Amadesi S, Reni C, Katare R, Meloni M, Oikawa A, Beltrami AP, Avolio E, Cesselli D,
582 Fortunato O, Spinetti G, et al. Role for substance P-based nociceptive signaling in progenitor

583 cell activation and angiogenesis during ischemia in mice and in human subjects. *Circulation*
584 (2012) 125:1774–1786. doi: 10.1161/CIRCULATIONAHA.111.089763

585 88. Wei JJ, Kim HS, Spencer CA, Brennan-Crispi D, Zheng Y, Johnson NM, Rosenbach M,
586 Miller C, Leung DH, Cotsarelis G, et al. Activation of TRPA1 nociceptor promotes systemic
587 adult mammalian skin regeneration. *Science Immunology* (2020) **5**:1–9. doi:
588 10.1126/SCIIMMUNOL.ABA5683

589 89. Donnelly DJ, Popovich PG. Inflammation and its role in neuroprotection, axonal regeneration
590 and functional recovery after spinal cord injury. *Experimental Neurology* (2008) doi:
591 10.1016/j.expneurol.2007.06.009

592 90. Hervera A, de Virgiliis F, Palmisano I, Zhou L, Tantardini E, Kong G, Hutson T, Danzi MC,
593 Perry RBT, Santos CXC, et al. Reactive oxygen species regulate axonal regeneration through
594 the release of exosomal NADPH oxidase 2 complexes into injured axons. *Nature Cell Biology*
595 (2018) **20**:307–319. doi: 10.1038/s41556-018-0039-x

596

597 10 Figure Legends

Figure 1. CCL21 is upregulated upon TRPV1⁺ nociceptive neuron activation. A. Graph showing the proportion of ChR2⁺ cells depending on the neuronal diameter. ChR2 is expressed in both large-diameter ($>35\mu\text{m}$) and small-diameter (35-15 μm) neurons. B. ChR2 expression in Thy1-ChR2 DRGs. Scale bar: 50 μm . C. Immunohistochemistry showing CCL21 expression in TRPV1⁺ neurons 2h after capsaicin injection. White arrows: magnified neurons in D. Scale bar: 50 μm . D. High magnification inset. E. Intraplantar capsaicin injection increased CCL21 expression in TRPV1⁺ nociceptors specifically as shown by mean fluorescence intensity (MFI) of TRPV1⁺ cells. a.u.: arbitrary units. Data are expressed as mean \pm s.e.m; Student's t-test; * $p < 0.05$; n=5-7 images.

Figure 2. CCL21 enhances DRG neurite outgrowth. A. *Ex vivo* CCL21 administration in the sciatic nerve promoted neurite outgrowth of DRG large-diameter neurons. Data are expressed as average neurite length per neuron \pm s.e.m; Student's t-test; ** p < 0.01; n=6 sciatic nerves. C. Dose-dependent increase in neurite length of *in vitro* CCL21-treated DRG large-diameter neurons. Data are expressed as average neurite length per neuron \pm s.e.m; One-way ANOVA, Bonferroni's post-hoc; * p < 0.05; n=3 wells. B-D. Tuj-1 representative immunostainings (B: *ex vivo* D: *in vitro*) after 24h in culture. Scale bar: 250 μ m.

Figure 3. CCR7 is required for CCL21-mediated DRG outgrowth. A. PV⁺ neurons express the canonical CCL21 receptor CCR7. Scale bar: 50µm. B. CCR7-blockade abolished the CCL21-dependent growth induction. Data are expressed as mean fold change of average neurite length per neuron vs each vehicle group±s.e.m. Two-way ANOVA, Bonferroni's post-hoc; ** $p < 0.01$ (vs IgG-veh); # $p < 0.05$; ## $p < 0.01$ (vs IgG-CCL21); n=8-9 images. C. Tuj-1 representative immunostainings after 24h in culture. Scale bar: 250µm.

Figure 4. Inhibiting the MEK-ERK pathway impairs the CCL21-dependent increased outgrowth. A. CCL21 and U0126, a MEK inhibitor, co-administration resulted in reduced neurite outgrowth compared to CCL21 administration alone. Data are expressed as average neurite length per neuron \pm s.e.m; Two-way ANOVA, Bonferroni's post-hoc; *** p < 0.001 (vs veh-DMSO), # p <

623 0.001 (vs CCL21-DMSO). n=7-12 images. B. Tuj-1 representative immunostainings after 24h in
624 culture. Scale bar: 250 μ m.

625 **Figure 5. CCL21 stimulates actin dynamics in the growth cone.** A. CCL21 administration resulted
626 in enlarged growth cones in large-diameter DRG neurons. White arrows: growth cones. Scale bar:
627 100 μ m. B. CCR7 expression is specially elevated in the growth cone. Scale bar: 50 μ m. C. Actin
628 branching is important for CCL21-dependent neurite outgrowth, as shown by impaired growth after
629 wiskostatin treatment. Data are expressed as average neurite length per neuron \pm s.e.m; One-way
630 ANOVA, Bonferroni's post-hoc; * p < 0.05; n=7-8 wells.

631 **Figure 6. Schematic representation of the proposed mechanism for a novel nociceptor-**
632 **proprioceptor dialogue leading to neuritic growth.** Activated TRPV1+ nociceptors secrete CCL21
633 which promotes actin branching in the growth cone of proprioceptor neurons. This mechanism is
634 mediated by the CCL21-CCR7 interaction, leading to a downstream activation of the MEK-ERK
635 pathway and final N-WASP-related actin cytoskeleton modifications.

636 **Suppl. Fig. 1. CCL19 administration does not induce neurite outgrowth.** Data are expressed as
637 average neurite length per neuron \pm s.e.m; n=8-12 images

638 **Suppl. Fig. 2. Pertussis toxin addition does not prevent the CCL21-dependent neurite**
639 **outgrowth increase.** Data are expressed as mean fold change of average neurite length per neuron vs
640 each vehicle \pm s.e.m; n=9-12 images.

Figure 1

A ChR2⁺ neurons
Size distribution

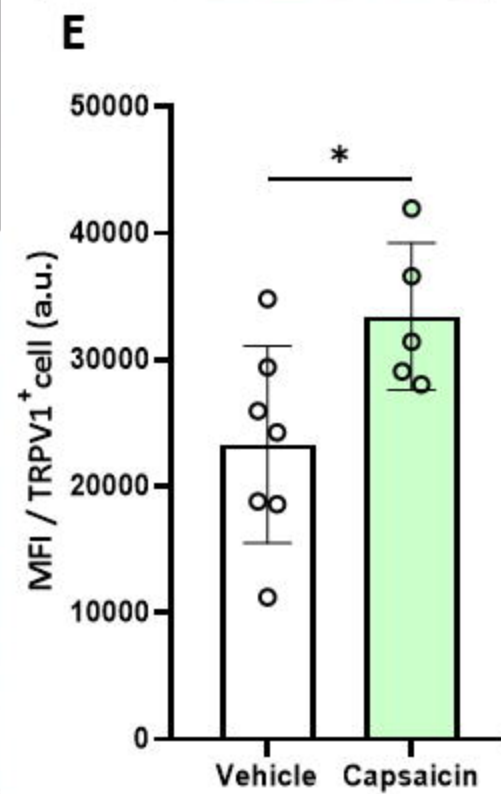
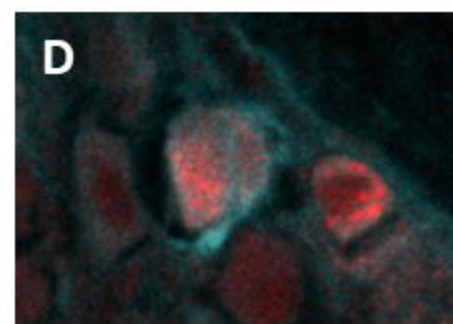
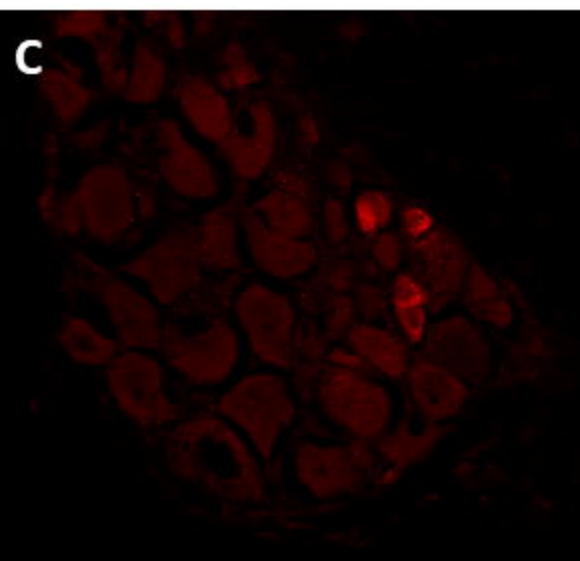
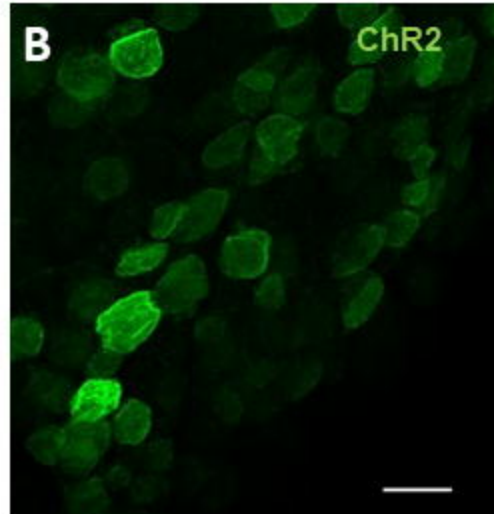
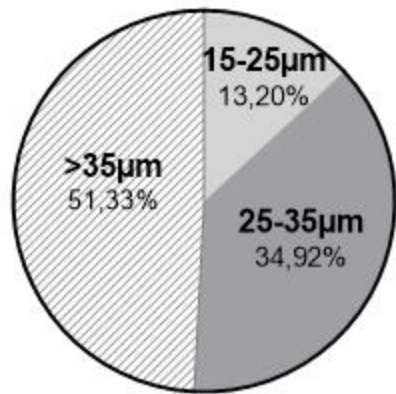


Figure 2

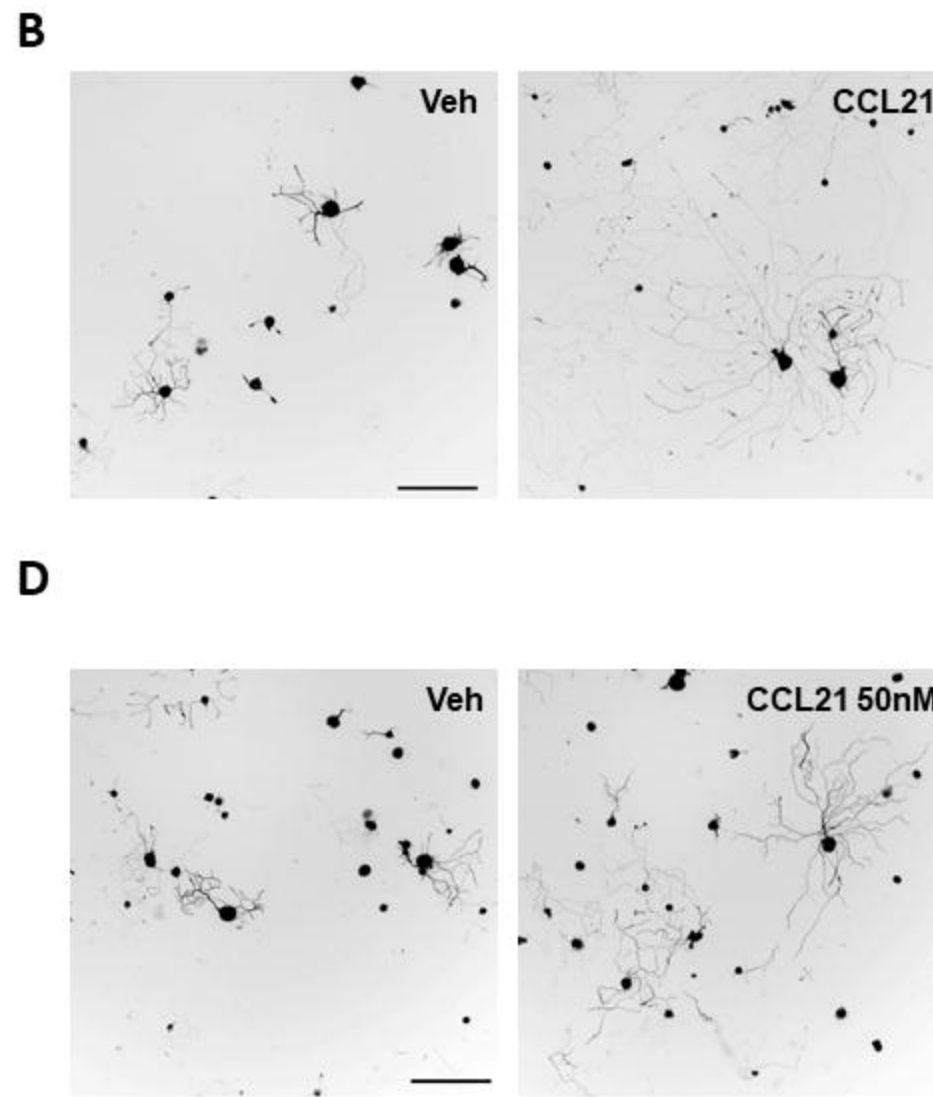
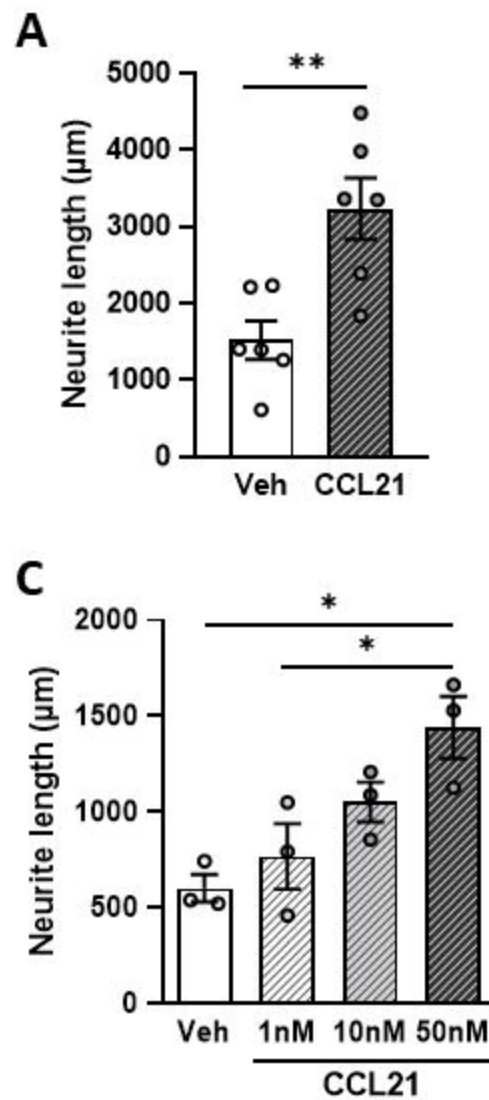


Figure 3

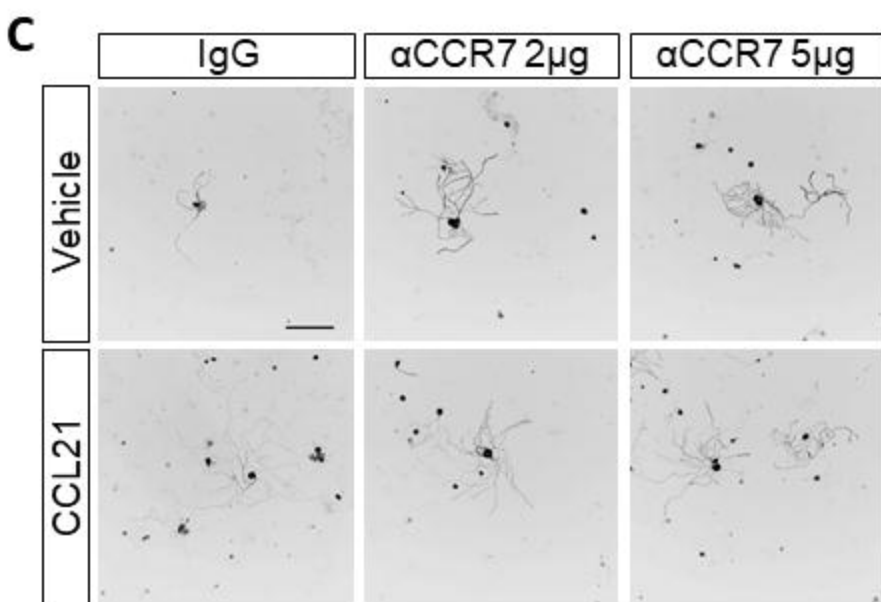
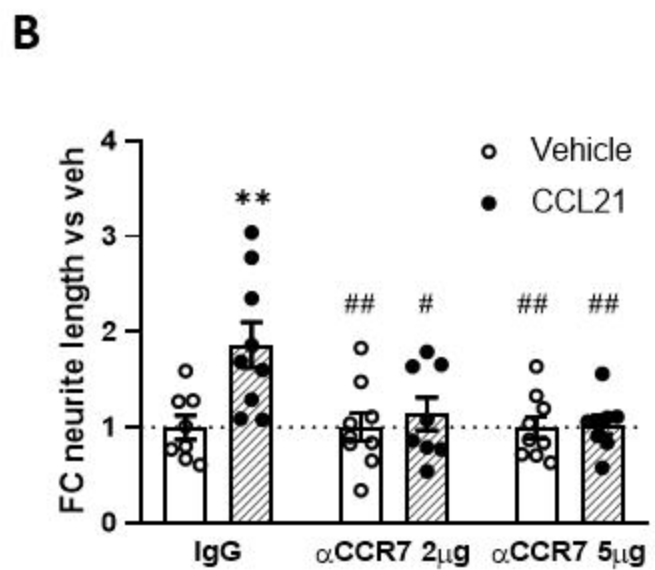
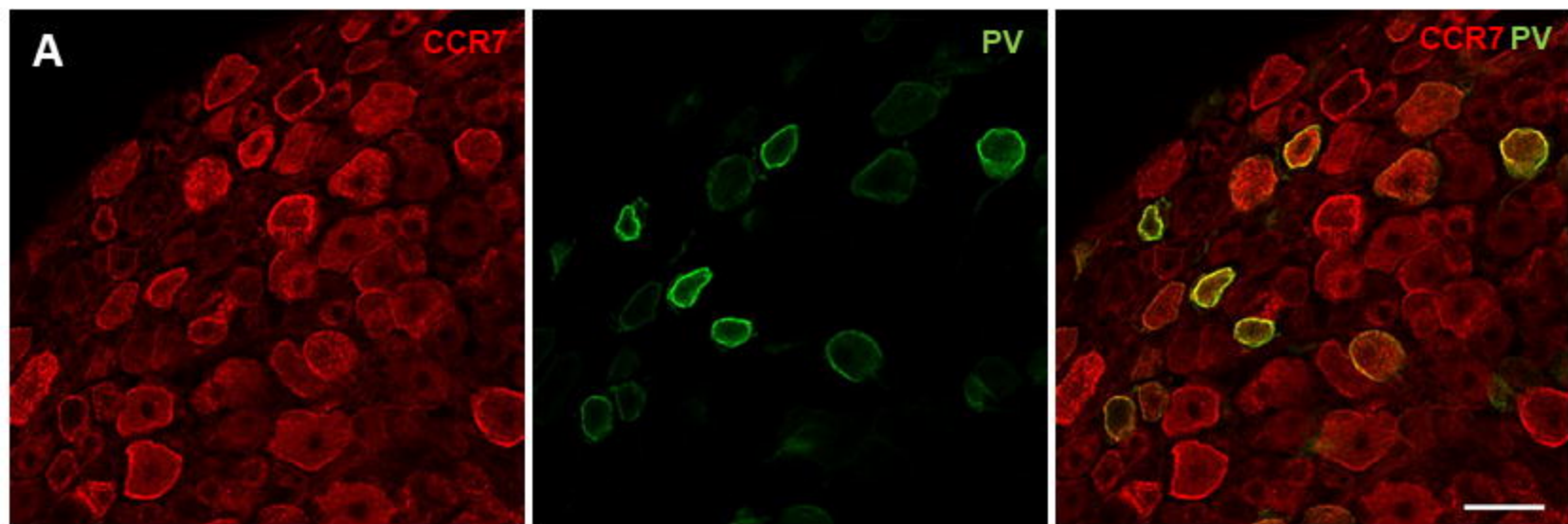
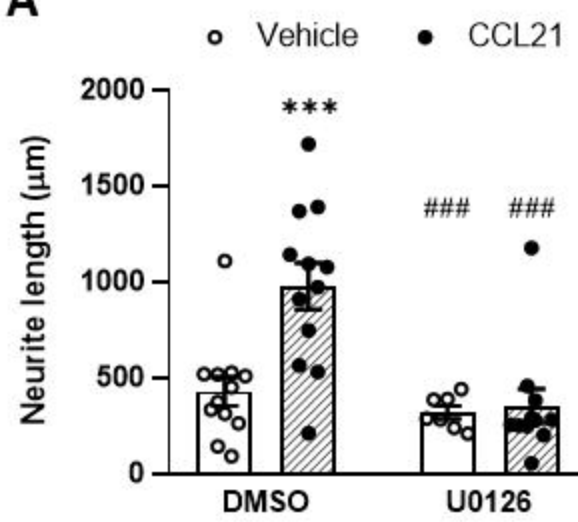


Figure 4

A



B

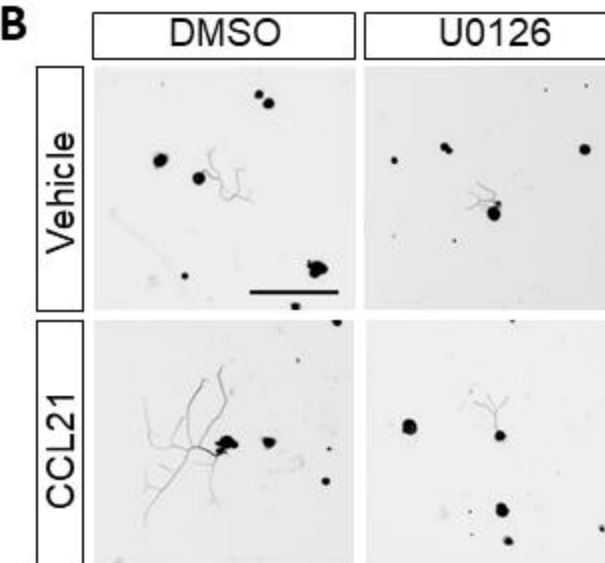
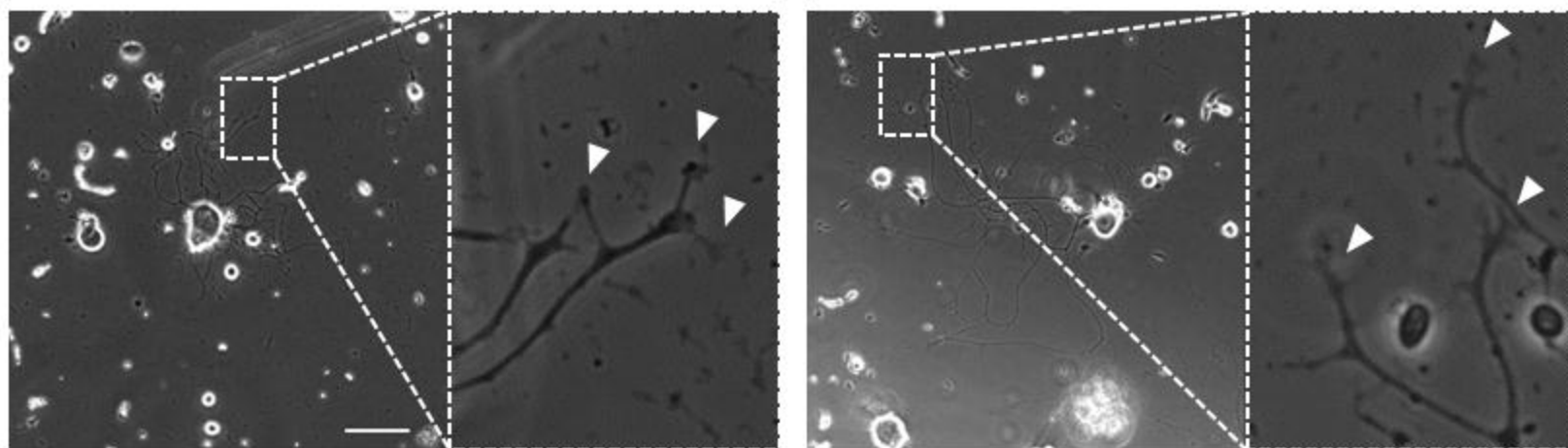


Figure 5

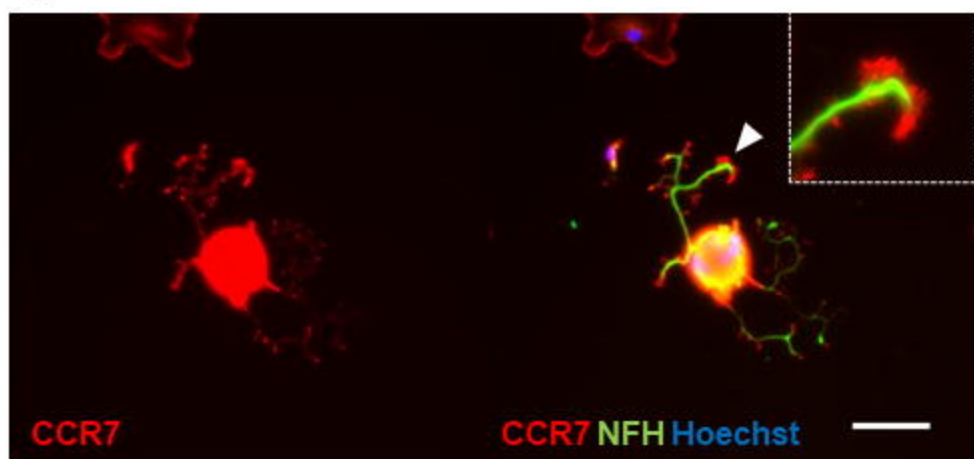
A

Vehicle

CCL21



B



C

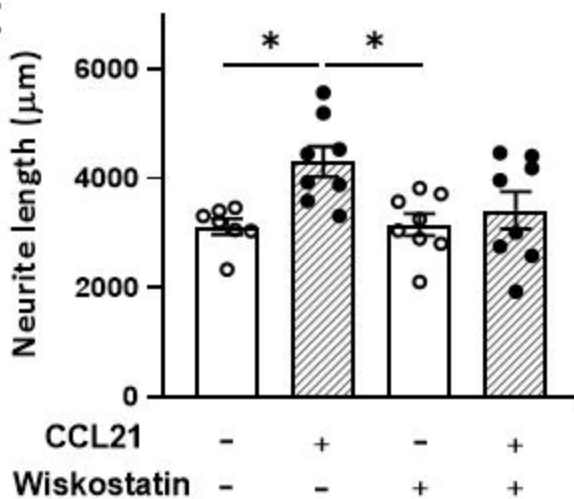


Figure 6

